JOURNAL OF PROPULSION AND POWER
Vol. 20, No. 2, March–April 2004

High-Speed, High-Temperature Finger Seal Test Results

Margaret P. Proctor*
NASA John H. Glenn Research Center at Lewis Field, Cleveland, Ohio 44135
Arun Kumar†
Honeywell Engines, Systems and Services, Phoenix, Arizona 85034
and
Irebert R. Delgado‡
U.S. Army Research Laboratory, NASA John H. Glenn Research Center at Lewis Field, Cleveland, Ohio 44135

A pressure balanced finger seal was tested in NASA's High-Temperature, High-Speed Turbine Seal Test Rig at conditions up to 922 K, 366 m/s, and 517 kPa to study its leakage, power loss, and wear performance at advanced engine conditions. Static, performance, endurance, and postperformance tests were conducted. The finger seal leakage performance met the flow factor goal of 7.72 kg-$\sqrt{}$K/MPa-m-s during the endurance test, which simulated expected advanced-engine rated power conditions. The maximum finger seal power loss of 10.4 kW occurred at 366 m/s and 517 kPa across the seal. Further design improvements are needed to reduce seal power loss. Finger seal power loss is comparable to measured brush seal power loss. Most finger seal wear occurred in the initial performance test and the accumulative seal weight loss leveled out over time. With approximately one-half the finger pad thickness remaining after 11 h of testing, the rate of seal wear is acceptable. Furthermore, the high velocity oxygen fuel thermally sprayed (HVOF) chrome carbide coating on the rotor performed well, with a final wear track depth less than 6.35 μm. The finger seal is very sensitive to clearance, and further testing is required to separate and quantify the effects of changes in radial clearance from apparent hysteresis.

Introduction

A VARIETY of seals are used by the gas turbine industry to contain and direct secondary flow into and around components for cooling and to limit leakage into and from bearing and disk cavities. The function of these seals is very important to the component efficiencies and attendant engine performance.[1] The Joint Turbine Advanced Gas Generator–phase 3 (JTAGG 3) program goals are to reduce overall engine specific fuel consumption by 40%, increase engine shaft horsepower to weight ratio by 120%, reduce production cost by 35%, and reduce maintenance cost by 35% (Ref. 2). The Integrated High Performance Turbine Engine Technology initiative, which the JTAGG 3 program supports, has set secondary flow system goals at 50% leakage reduction for phase 2 and 60% reduction for phase 3.[3] Improved seals will be needed to reach these goals. An advanced seal leakage flow factor goal is set at 7.72 kg-$\sqrt{}$K/MPa-m-s, which is less than half the flow factor calculated for a four-knife labyrinth seal with a radial clearance of 254 μm (Ref. 4). Flow factor is defined later in the text.

The finger seal is an innovative design recently patented[5] by AlliedSignal Engines, which has demonstrated considerably lower leakage than commonly used labyrinth seals and is considerably cheaper to manufacture than brush seals. The cost to produce finger seals is estimated to be about half of the cost to produce brush seals.[4] In previous testing, measured finger seal leakage flow factor was 20–70% less than that calculated for a typical four-knife labyrinth seal with a 127-μm radial clearance.[4] Furthermore, experimentally measured leakage flow factors for brush seals[6] are similar to those of finger seals.[4] Replacing labyrinth seals with finger seals at locations that have high pressure drops, typically main engine and thrust balance seals, can reduce air leakage at each location by 50% or more. This directly results in a 0.7–1.4% reduction in specific fuel consumption and a 0.35–0.7% reduction in direct operating cost.[4]

In the late 1990s a low cost, pressure-balanced, low hysteresis finger seal was developed and successfully demonstrated at operating conditions of 237 m/s, 414 kPa, and 811 K and 288 m/s, 552 kPa, and 700 K. Both the seal and rotor were in excellent condition after 120 h of endurance testing.[4] This pressure balanced finger seal was also patented by AlliedSignal, Inc., in 2001.[7] The finger seal is a contacting seal, which raises concern about the heat it will generate and its life capability at the higher temperatures and speeds required for advanced engines. To address this concern, a pressure-balanced, low-hysteresis finger seal was tested at operating conditions up to 366 m/s, 517 kPa, and 922 K (1200 fps, 75 psid differential and 1200°F). These are the first test results obtained with NASA's new High-Temperature, High-Speed Turbine Seal Test Rig. The test hardware, apparatus, and experimental procedures will be described followed by a discussion of the seal performance and wear results.

Test Hardware

With a design criteria developed during earlier testing of various finger seal configurations, a low-hysteresis finger seal was designed and fabricated for testing at advanced engine operating conditions. The low-hysteresis, pressure-balanced seal design features developed in Ref. 4 were incorporated in this design.

The finger seal is similar in general configuration to a brush seal, but functions in a different manner. Instead of a random array of fine wires, the finger seal uses a stack of tight-tolerance sheet stock elements. Each element is machined to create a series of slender curved beams or fingers around the inner diameter (Fig. 1). Each of these fingers 7 has an elongated contact pad 6 at its free end (Fig. 1). Each element 1 also has a series of assembly hole pairs 8 near its outer diameter. These holes are for the rivets 5 that assemble the seal. The holes are spaced such that when the elements are alternately indexed to the two holes, the spaces between the fingers of one element are covered by the fingers of the adjacent element. Usually a seal is assembled with multiple finger elements 1, forward and aft spacers 2, and forward cover plate 3 and aft cover plate 4 (Fig. 1). The seal is fitted over the rotating shaft or rotor with a small amount of clearance or interference, depending on the application.

Received 23 September 2002; revision received 27 June 2003; accepted for publication 5 July 2003.

*Aerospace Engineer, Mechanical Components Branch.
†Principal Engineer, Mechanical Systems, Structures and Dynamics, 111 S. 34th Street. Member AIAA.
‡Mechanical Engineer, Mechanical Components Branch.

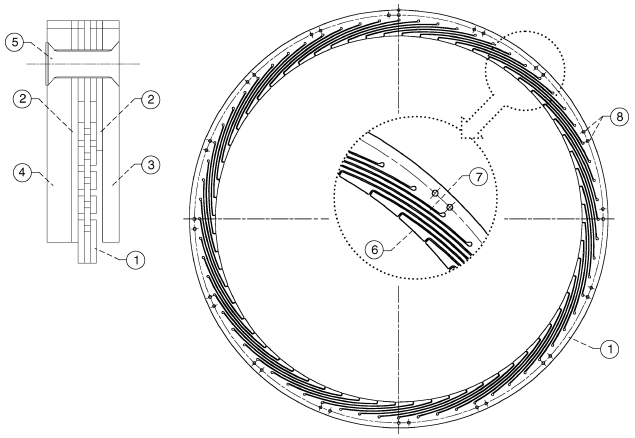

Fig. 1 Finger seal design: 1, finger element; 2, spacer; 3, forward cover plate; 4, aft cover plate; 5, rivet; 6, finger contact pad; 7, finger; and 8, indexing and rivet holes.

The staggered finger/pad features as well as the radial contact between the rotating land and the pads impede airflow through the seal. The flexible fingers can bend radially to accommodate shaft excursions and relative growth of the seal and rotor resulting from rotational forces and thermal mismatch.

A key feature of the finger seal is its low cost of manufacture. The geometric features on the seal laminates are fashioned using wire electric discharge machining, which is extremely cost effective. Sheet stock of various alloys and thickness required for the seals is readily available. Riveting of the assembly does not require any elaborate tooling or assembly process.

A parametric finite element modeling program and Honeywell proprietary programs were used to optimize the finger seal design. The finger seal tested was sized to run with a slight interference at operating conditions. The finger elements, spacers, and side plates are made of sheet AMS5537. This is a cobalt-base alloy that combines good formability and excellent high-temperature properties. It displays excellent resistance to the hot corrosive atmospheres encountered in jet engine operations.

The 21.6-cm- (8.5-in.-) diam test rotor is made of MAR–M–247, a nickel-base alloy with excellent high-temperature properties. The seal runner surface on the rotor is coated with chrome carbide using high-velocity oxygen fuel thermal spraying.

Test Apparatus

Turbine Seal Test Rig

Testing was conducted in the NASA high-temperature, high-speed turbine seal test rig shown in Fig. 2 and located at the NASA John H. Glenn Research Center in Cleveland, Ohio. The turbine seal test rig consists of a 21.6-cm-diam test rotor mounted on a shaft in an overhung configuration. The shaft is supported by two oil-lubricated bearings. A balance piston controls the axial thrust load on the bearings due to pressure loads on the test rotor. An air turbine drives the test rig. A torquemeter is located between the air turbine and the test rig and is connected to each by quill shafts. The test seal is clamped into the MAR–M–247 seal holder as shown in Fig. 3. A C-seal located at the seal holder/test seal interface prevents flow from bypassing the test seal at its outer diameter. The seal holder is heated to approximately match the thermal growth of the rotor and prevent a damaging change in radial clearance. Heated, filtered air enters the bottom of the test rig and passes through an inlet plenum that directs the heated air axially toward the seal/rotor interface. The hot air either leaks through the test seal to the seal exhaust line or exits the rig before the test seal through a controlled bypass line at the top of the rig. If seal leakage is low, the bypass line must be open to maintain sufficient flow through the test rig to keep the rig hot. The seal exhaust line vents to atmosphere. The seal exit pressure was nominally 7–14 kPa above atmospheric pressure due to backpressure from the bearing cavity purge air.

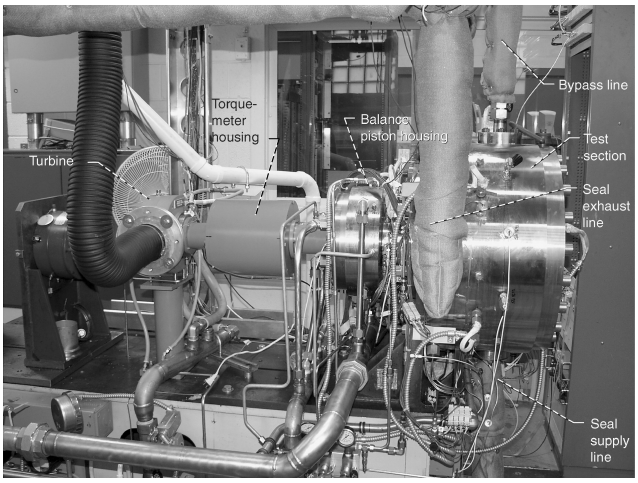

Fig. 2 High-Temperature, High-Speed Turbine Seal Rig.

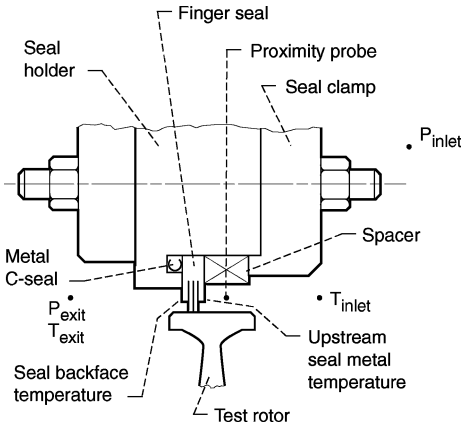

Fig. 3 Test seal configuration and location of research measurements.

Instrumentation

Seal inlet and exit temperatures and static pressures, seal upstream metal temperature, and seal backface temperatures were measured at the locations shown in Fig. 3. For each measurement there were three probes equally spaced around the circumference, except for the upstream seal metal temperature for which two thermocouples were located at the 90- and 180-deg positions; 0 deg is top dead center. Type-K thermocouples were used and all were 1.6 mm, Inconel sheath, closed ball except the seal exit temperatures, which were 3.2 mm diameter, and the seal metal and backface temperatures, which were open ball.

High-temperature, capacitance proximity probes were mounted in the seal holder at four, equally spaced locations to view the test rotor outer diameter. These probes were used to measure the change in clearance between the seal holder and the rotor and to monitor the rotordynamic behavior of the test rotor. The average inlet air temperature is used as the probe temperature when correcting the probe output. These proximity probes have an accuracy of 5 μm, at room temperature.

Annubar flow meters are used to measure the flow rates of the hot air supplied to the rig and the air exiting the rig through the bypass line. The seal leakage is the difference between these two flow measurements. The seal leakage rate is then used to calculate the flow factor, which is defined as

$$\Phi = \frac{\dot{m}\sqrt{T_{\text{av}} + 459.60}}{P_u \times D_{\text{seal}}}$$

where

$\dot{m}$ = air leakage flow rate, kg/s
T_{av} = average seal air inlet temperature, K
P_u = air pressure upstream of seal, MPa
D_{seal} = outside diameter of the seal rotor, m

The flow factor can be used to compare the leakage performance of seals with different diameters and with different operating conditions. The accuracy of the measured flow factor is ±1.5%.

A phase shift torquemeter measures the total torque of the seal test rig. It has a feature to compensate for any relative motion between the torsion shaft and stator. The torquemeter is rated to 22 N · m and has a maximum operating speed of 5236 rad/s and an absolute accuracy of 0.13% or 0.028 N · m. The seal torque is the rig torque with the test seal installed minus the rig tare torque. The rig tare torque was measured at various inlet air temperatures and speeds with no seal installed. This data was two dimensionally curve fitted. The fitted curve is used with the measured average inlet air temperature and speed to infer the corresponding tare torque. Seal power loss is simply the seal torque multiplied by speed. The maximum error in the seal power loss measurements is 98 W over the range of test conditions. The speed measurement from the torquemeter is accurate to <0.04% or 1.4 rad/s, at the maximum speed tested.

Experimental Procedures

Four tests were performed: a static leakage test, a performance test, an endurance test, and a postendurance performance test.

A static test was performed at ambient temperature, 700 K, and 922 K to obtain baseline leakage data. At steady conditions, seal leakage data was taken for 1 min at steady seal differential pressures from 0 to 517 kPa and then from 517 to 0 kPa.

Seal performance test data were taken at average inlet air temperatures of 700, 866, and 922 K. At each temperature, differential pressures of 69, 276, and 517 kPa were applied, and at each pressure, surface speed was stepped up and down as follows: 0, 183, 274, 366, 274, 183, and 0 m/s. Data were recorded every second for approximately 30 s after reaching a steady state at all test conditions, except for the first test condition of 700 K and 69 kPa for which data were continuously recorded every second to observe the initial wearing of the seal. The seal and rotor were inspected after the performance test was completed. The endurance test assessed the ability of the seal to maintain low leakage over an extended period of time. This test was conducted at 922 K, 366 m/s, and 517 kPa for 4 h at which time the seal leakage and power loss stopped changing. The seal and test rotor were removed for inspection after 1, 2, and 4 h of testing. The performance test was repeated after the endurance test.

Seal Performance Results

Initial Static Test

The static performance of the finger seal at an average inlet air temperature of 922 K is shown in Fig. 4 as flow factor vs pressure drop across the seal. The flow factor increases with pressure drop until about 103 kPa and then levels off at a flow factor of approximately 2.9 kg-$\sqrt{}$K/MPa-m-s. At this point the flow is choked.

Performance Test

Initial Rotation

The finger seal was tested at 700-K average inlet air temperature and 69 kPa across the seal. Data were recorded once a second while the speed was stepped up to obtain 183-, 274-, and 366-m/s surface velocities and then stepped back down to 274, 183, and 0 m/s. Figure 5 shows time history for shaft speed, seal power loss, average seal backface and inlet air temperatures, and radial seal clearance for this initial rotation. The seal power loss shown is the total power minus the steady-state tare power. The positive and negative spikes as each speed level is attained are largely due to acceleration and deceleration inertia. Note that at 366 m/s the steady-state seal power loss declines as time at condition increases. This could indicate wearing of the seal. At steady-state conditions, the seal power loss did not exceed 2.1 kW. Frictional heating due to seal-to-rotor contact and wearing is also evident in the average seal backface and inlet air temperatures time history. As speed is decreased, both the seal power loss and average seal backface temperature levels are lower than during the speed increase, which might also indicate that wear has occurred. The centrifugal growth of the rotor can be seen in the time history of the radial seal clearance. The radial clearance shown in Fig. 5 is the change in the distance between the seal holder and the rotor from ambient, static conditions, plus the initial clearance between the seal and the rotor at ambient temperature. This clearance is not necessarily the clearance between the fingers and the rotor. From 0 to 366 m/s, the radial interference increased from 81 to 249 μm, a change of 168 μm, which exceeds the expected centrifugal growth of about 84 μm. This indicates that the seal holder and rotor are not maintaining the same temperature, which is supported by the approximately 111-K change in the seal backface temperature during this initial rotation.

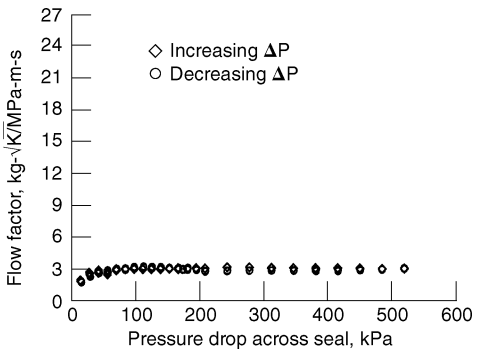

Fig. 4 Static leakage performance of finger seal at average seal inlet air temperature of 922 K.

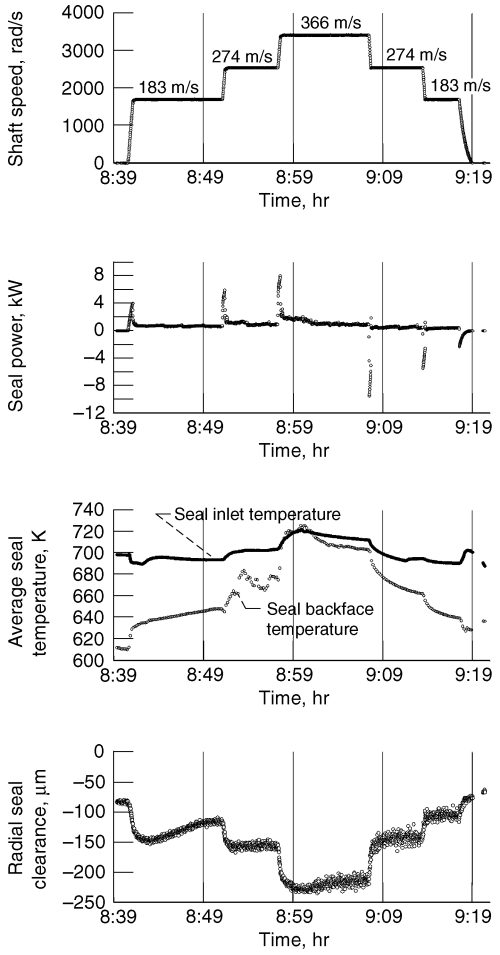

Fig. 5 Time history of initial rotation at 700-K average seal inlet air temperature and 69-kPa pressure drop across seal.

Leakage

The finger seal leakage performance at average seal inlet air temperatures of 700 and 922 K is shown in Figs. 6 and 7, respectively,

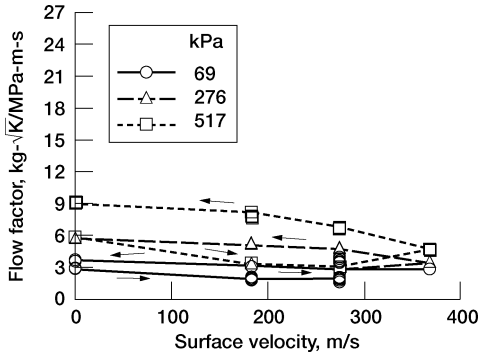

Fig. 6 Finger seal performance test data at 700-K average seal inlet air temperature and 69-, 276-, and 517-kPa pressure drop across seal.

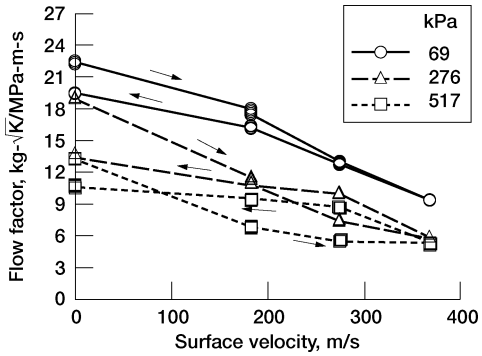

Fig. 7 Finger seal performance test data at 922-K average seal inlet air temperature and 69-, 276-, and 517-kPa pressure drop across seal.

as flow factor vs surface velocity at pressure drops across the seal of 69, 276, and 517 kPa. At 700 K, it can be seen that the flow factor at 69 kPa is less than at 276 and 517 kPa. Also, the flow factor data at 69 kPa and for increasing speed at 276 and 517 kPa are about the same, approximately 3.1–3.5 kg-$\sqrt{}$K/MPa-m-s. Hysteresis can be seen in the data taken at 276 and 517 kPa and is more pronounced at 517 kPa. When speed increases, the centrifugal growth of the rotor pushes the fingers radially away. When speed decreases and the rotor diameter shrinks, the fingers may remain in their outer position, causing leakage and flow factor to increase. Hysteresis may also be due to rapid wear of the seal during initial shaft rotation, which would increase the seal clearance. Likewise, seal holder and rotor temperature changes can affect the seal clearance and appear as hysteresis.

The flow factor for an average inlet air temperature of 922 K is shown in Fig. 7. At all three pressure differentials, the flow factor decreases as speed increases due to the centrifugal growth of the rotor reducing the clearance, as expected. Again, hysteresis is evident, but at 69 and 276 kPa there is an inconsistency with earlier data in that flow factor is lower for decreasing speed than for increasing speed. Also, as pressure drop across the seal increased, flow factor decreased, which is opposite to what happened at 700 K. This can be explained by a look at the corresponding radial clearance data in Fig. 8. It shows that the radial clearance is lower for decreasing speed compared to increasing speed and that the radial clearance decreases as pressure drop across the seal increases. In this test sequence there is a clear and definite influence of changes in the radial clearance between the seal holder and the seal rotor. Although data were taken at steady-state conditions, the clearance between the seal holder and the rotor was not a controlled parameter. It seems that some of the hysteresis observed may actually be due to changes in the radial clearance between the seal holder and rotor and not due to the fingers getting stuck in the open position. The clearance data shown here indicate that a radial interference existed between the seal and rotor for most of the performance testing. By the end of the performance test, the seal had worn such that a clearance existed between it and the rotor at ambient conditions. However, at both

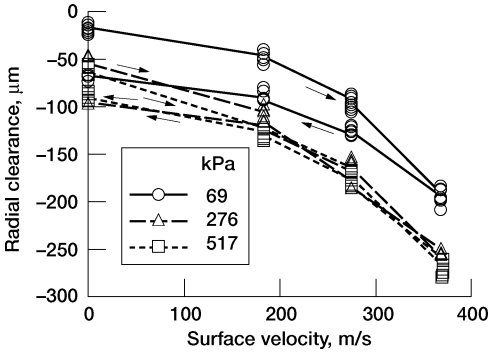

Fig. 8 Finger seal performance test radial clearance data at 922-K average seal inlet air temperature and 69-, 276-, and 517-kPa pressure drop across seal.

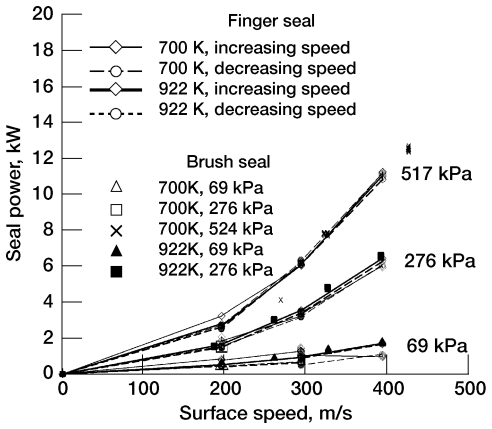

Fig. 9 Finger seal and brush seal power loss vs speed at 700- and 922-K average seal inlet air temperature and 69-, 276-, and 517-kPa pressure drop across seal.

average seal inlet air temperatures of 700 and 922 K, the finger seal had a flow factor less than the goal of 7.72 kg-$\sqrt{}$K/MPa-m-s for the maximum operating conditions (517 kPa and 366 m/s).

Power Loss

The finger seal power loss is shown in Fig. 9 as a function of speed for the performance data taken at 700 and 922 K average inlet air temperature and 69, 276, and 517 kPa. There is no significant difference between the data for 700 and 922 K. As expected, the seal power loss increased with speed and also increased as pressure drop across the seal increased due to pressure loading. Pressure loading occurs because the outer surface of the finger is longer than the inner surface, which under uniform pressure results in a net force pushing the fingers in toward the rotor. Although the upstream finger element experiences uniform pressure loading, the pressure loading on the middle and downstream finger elements is not precisely known. The finger seal power loss at 366 m/s was 1.5, 6, and 10.4 kW at 69, 276, and 517 kPa across the seal, respectively. The measured power loss was in good agreement with analytical predictions made by Honeywell using a proprietary code. A brush seal with a similar radial interference as this finger seal was also tested, and its measured power loss is also shown in Fig. 9. The brush seal power loss is very similar to the finger seal power loss. Unfortunately the corresponding leakage data for the brush seal tested was not obtained due to an instrumentation problem.

Endurance Test

The time history of key parameters for the endurance test is shown in Fig. 10. Surface speed and pressure drop across the seal are very stable over the run: 366 ± 0.15 m/s and 517 ± 0.62 kPa. There is some small fluctuation in the flow factor, average inlet air temperature, and radial clearance, and they correlate with each other. The

Table 1 Comparison of first and last performance test flow factors at 366 m/s

Pressure drop across seal, kPa	Average inlet air 700 K			Average inlet air 866 K			Average inlet air 922 K		
	69	276	517	69	276	517	69	276	517
Flow factor first test	2.9	3.28	4.83	6.76	5.0	4.8	9.65	5.8	5.6
Flow factor last test	9.65	8.11	8.30	13.1	9.07	7.72	15.8	11.4	9.1
Last ϕ/first ϕ	3.33	2.47	1.72	1.94	1.81	1.6	1.64	1.97	1.62

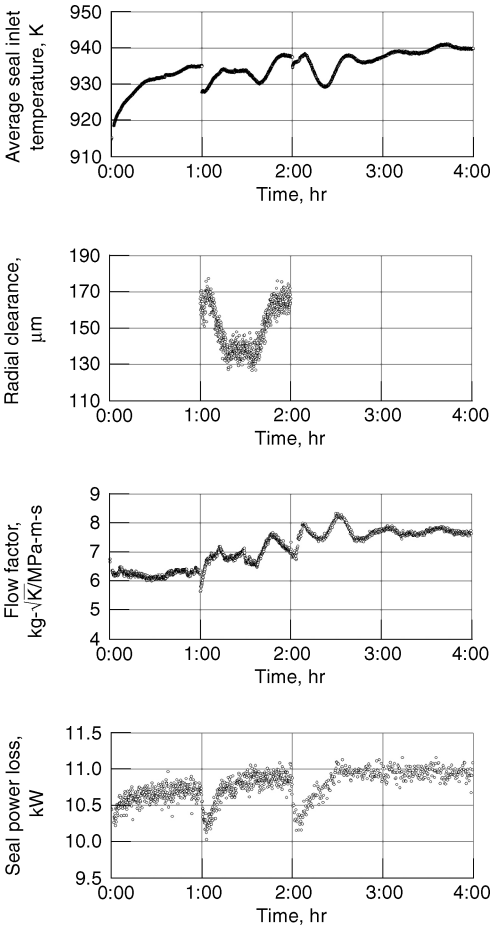

Fig. 10 Time history of finger seal endurance test at 922-K average seal inlet air temperature, 366-m/s surface speed, and 517-kPa pressure drop across seal.

absence of radial clearance data for the first hour and last two hours of the endurance test is due to problems with the proximity probe instrumentation. Seal power loss initially climbs and then levels out. The minimal change in flow factor over the duration of the miniendurance test indicates that most of the wear of the seal occurred during the prior performance test. The final flow factor level of 7.72 kg-$\sqrt{}$K/MPa-m-s meets the leakage performance goal. Assuming isentropic, compressible, choked nozzle flow, the finger seal performed in the endurance test as though it had an equivalent radial clearance of 61 μm, which is much less than the clearance required by a noncompliant, noncontacting seal. It was also observed that the inlet air temperatures measured at three locations around the seal showed a more uniform temperature around the seal than during the performance test. In the endurance test, the seal inlet temperature at the top of the rig was about 28 K lower than at the 120- and 240-deg locations, compared to 56–83 K for the performance test. This was largely due to the long period of time at constant conditions.

Figure 10 shows a flow factor of approximately 7.72 kg-$\sqrt{}$K/MPa-m-s at 922 K, 517 kPa, and 366 m/s after 4 h of endurance testing. This is very similar to the low leakage results for a 13-cm-diam pressure-balanced finger seal design tested at 811 K, 414 kPa, and 237 m/s in Ref. 5.

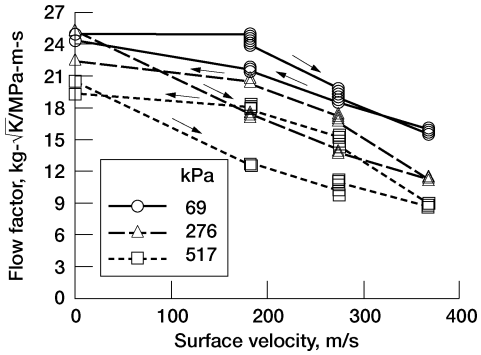

Fig. 11 Postendurance performance test; finger seal flow factor vs speed at 922-K average seal inlet air temperature and 69-, 276-, and 517-kPa pressure drop across seal.

Postperformance Test

The performance test was repeated after the endurance test. Hysteresis was present in all of the data taken at 700, 866, and 922 K. Again, the flow factor decreased as speed increased due to the centrifugal growth of the rotor, and the pressure closing effect was evident in all cases. A comparison of the flow factors from the first and last performance tests at 366 m/s for all average inlet air temperatures and pressure drops across the seal is given in Table 1. The flow factors after the endurance test were 1.6 to 3.33 times those in the first performance test. The largest increase occurred between the initial data taken at 700 K and 69 kPa due to the wearing in of the seal.

The flow factors measured at an average inlet air temperature of 922 K are shown as a function of speed at pressure differentials of 69, 276, and 517 kPa in Fig. 11. The flow factors ranged from 8.7 to 25.1 kg-$\sqrt{}$K/MPa-m-s. The hysteresis is somewhat worse in this last performance test than in the first performance test. As seen in the first 922 K performance test, the hysteresis is reversed at 69 kPa with the flow factor for decreasing speed being lower than for increasing speed. This is likely due to changes in the radial clearance, however, the proximity probes stopped working during this test, and the data were not available to confirm the effect. At the maximum operating conditions (922 K, 366 m/s, and 517 kPa) the measured flow factor of 9.1 kg-$\sqrt{}$K/MPa-m-s is only slightly higher than the goal of 7.72 kg-$\sqrt{}$K/MPa-m-s.

The finger seal power loss measured during the postendurance performance test is slightly less and very comparable to the measurements made in the first performance test as can be seen by comparing Fig. 12 to Fig. 9, respectively.

Wear Results

Seal Wear

The majority of the observed finger seal wear most likely occurred during the initial performance test, when the seal initial radial interference of 165 μm changed due to centrifugal growth of the rotor and due to the pressure closing effect of the finger design.

Figure 13 shows the accumulated seal weight loss after the first performance test (3.5 h), first, second, and fourth hour of endurance testing, and final performance test (11.0 h). Over 70% of the total seal weight loss occurred during the first performance test. The remaining 30% was spread out in the remaining endurance and final performance tests. The seal weight loss appears to converge asymptotically toward a steady-state value. When it is assumed that this weight loss occurred uniformly around the circumference of the

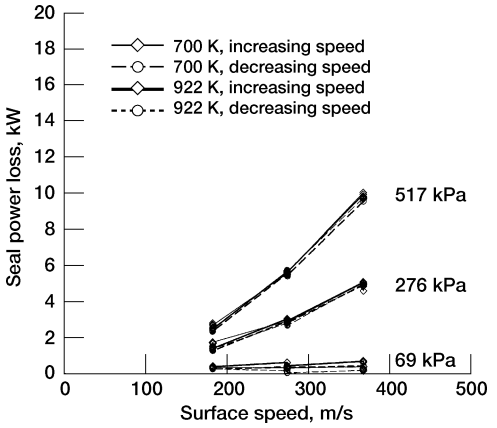

Fig. 12 Postendurance performance test; finger seal power loss vs speed at 922-K average seal inlet air temperature and 69-, 276-, and 517-kPa pressure drop across seal.

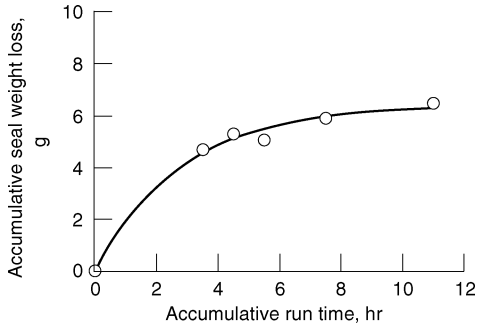

Fig. 13 Finger seal accumulative weight loss vs accumulative run time.

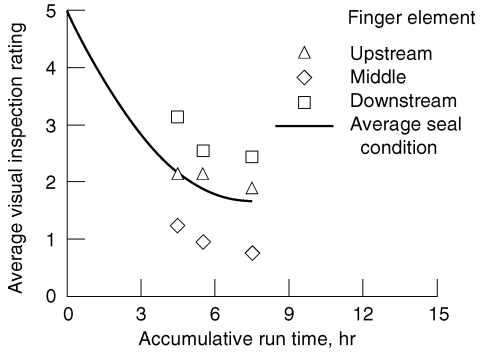

Fig. 14 Average visual inspection rating of finger seal wear vs accumulative run time for upstream, middle, and downstream finger elements: 5 = 0% average pad wear, 4 = 25% average pad wear, 3 = 50% average pad wear, 2 = 75% average pad wear, 1 = 100% average pad wear, and 0 = no pad.

seal, the radial wear is calculated to be about 889 μm, or slightly more than half the finger pad thickness.

The visual inspection of the individual finger pads also suggests that minimal seal weight loss occurred after the first performance test. All 64 pads on each of the 3 laminates were given a qualitative rating (0–5 scale) based on the amount of radial wear seen. For example, a 5 was given if the pad showed very little wear. A 3 was given for pads showing approximately 50% radial wear. A 1 was given if the pad toe was worn to a point. The 64 individual pad ratings were averaged to give an overall rating for each laminate. Figure 14 shows the averaged visual laminate wear rating for the three laminates of the finger seal after 1, 2, and 4 h of endurance testing. The average laminate wear rate for each laminate decreases asymptotically to a steady-state value. Note that the middle laminate was observed to have the worst overall wear of the three laminates. This result is not understood. Further analysis of the pressure balance

Table 2 Average rotor wear track measurements

Test type	Width, μm	Depth, μm
Baseline	0	——
First performance	2413	6.22
First-hour endurance	2108	4.47
Second-hour endurance	2642	4.19
Fourth-hour endurance	2413	6.32
Second performance	2438	5.49

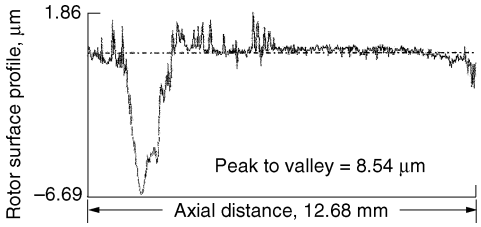

Fig. 15 Typical profile of seal wear track on rotor outer diameter.

geometry and its pressure loading effect on each laminate, along with the frictional forces on the side faces, is needed. The qualitative visual inspection ratings correspond reasonably well with the radial wear calculated from the weight loss.

Rotor Wear

Rotor wear was quantified using a profilometer. A typical profile of the wear track is shown in Fig. 15. Eight measurements were taken around the circumference of the rotor to determine an average track width and depth. These averages are presented in Table 2 for each inspection. Both the track width and track depth measurements indicate that the majority of the seal wear took place during the first performance test. The average track width ranged from 2032 to 2540 μm, and the average track depth ranged from 3.81 to 6.35 μm. This is a small and acceptable amount of wear. The scatter in the data is likely due to the uncertainty in taking the measurements at the same circumferential location on the rotor for each inspection. The circumferential locations were visually sighted using the bolt hole locations and etch marks as guides. Given that the performance test effectively covers the entire range of temperatures, pressures, and surface speeds that the seal would be subjected to during the test program, it is likely that the overall seal track width was worn in during this first performance test.

Conclusions

Overall the finger seal performed well and holds promise for use in advanced engines. After careful review of the test results the following conclusions are made.

1) The finger seal leakage is very sensitive to clearance.

2) The finger seal leakage performance met the flow factor goal of 7.72 kg-$\sqrt{}$K/MPa-m-s during the endurance test, which simulated expected advanced-engine rated power conditions.

3) The finger seal exhibited some hysteresis, some of which may actually be due to changes in the radial clearance between the seal holder and the test rotor. Further testing is required to separate and quantify the effects of changes in radial clearance from any hysteresis.

4) The maximum finger seal power loss, which occurred at 366 m/s and 517 kPa across the seal, was 10.4 kW. Further design improvements need to be made to reduce the seal power loss.

5) Finger seal power loss is comparable to the brush seal power loss.

6) Given that most of the finger seal wear occurred in the initial performance test, that the accumulative seal weight loss leveled out over time, and that approximately one-half the finger pad thickness remained after the tests were complete, the rate of seal wear is acceptable. Furthermore, the high velocity oxygen fuel thermally sprayed (HVOF) chrome carbide coating on the rotor performed well inasmuch as it had a final wear track depth less than 6.35 μm, which is only about 2.5% of the coating thickness, after 11 h of testing.

Acknowledgments

The authors acknowledge the contributions of the NASA John H. Glenn Research Center at Lewis Field, Cleveland, Ohio, where all testing was conducted, particularly the leadership of Bruce M. Steinetz, who guided the design, procurement, and fabrication of the new High-Temperature, High-Speed, Turbine Seal Test Rig. The authors also thank William A. Troha, Raymond J. Knorr, Eduardo R. Guerra, Eric B. Bridges, and Donald L. Glick of Honeywell Engines, Systems and Services for their dedicated support in program management and engineering support.

References

[1]Steinetz, B. M., Hendricks, R. C., and Munson, J., "Advanced Seal Technology Role in Meeting Next Generation Turbine Engine Goals," NASA TM 1998-206961, April 1998.

[2]Hirschberg, M., "On the Vertical Horizon: IHPTET—Power for the Future," VERTIFLITE, The American Helicopter Society, Alexandria, VA, Spring 2000, pp. 36–38.

[3]Mayhew, E. R., Bill, R. C., Voorhees, W. J., and O'Donnell, J., "Military Engine Seal Development: Potential Dual Use," AIAA Paper 94-2699, June 1994.

[4]Arora, G. K., Proctor, M. P., Steinetz, B. M., and Delgado, I. R., "Pressure Balanced, Low Hysteresis, Finger Seal Test Results," NASA TM 1999-209191, June 1999; also AIAA Paper 99-2686, June 1999.

[5]Johnson, M. C., and Medlin, E. G., "Laminated Finger Seal with Logarithmic Curvature," U.S. Patent 5,108,116, April 1992.

[6]Arora, G. K., and Proctor, M. P., "JTAGG II Brush Seal Test Results," NASA TM 107448, July, 1997; also AIAA Paper 97-2632, July 1997.

[7]Arora, G. K., and Glick, D. I., "Pressure Balanced Finger Seal," U.S. Patent 6,196,550, March 2001.